

# Inhibition of *Escherichia coli* respiratory enzymes by short visible femtosecond laser irradiation

Chieh-Han Lu<sup>1</sup>, Kung-Hsuan Lin<sup>2</sup>, Yung-Yuan Hsu<sup>1</sup>, Kong-Thon Tsen<sup>3</sup>,  
Yung-Shu Kuan<sup>4,5</sup>

<sup>1</sup>Department of Physics, National Taiwan Normal University, Taipei, 11677, Taiwan

<sup>2</sup>Institute of Physics, Academia Sinica, Taipei 11529, Taiwan

<sup>3</sup>Department of Physics, Arizona State University, Tempe, AZ 85287, USA

<sup>4</sup>Institute of Biochemical Science, National Taiwan University, Taipei, 10617, Taiwan

<sup>5</sup>Institute of Biological Chemistry, Academia Sinica, Taipei 11529, Taiwan

E-mail: [yskuan@ntu.edu.tw](mailto:yskuan@ntu.edu.tw) (Y.S. Kuan); [896410079@ntnu.edu.tw](mailto:896410079@ntnu.edu.tw) (C.H. Lu).

## Abstract:

Visible femtosecond laser is shown to be capable of selectively inactivating a wide spectrum of microorganisms in a wavelength and pulse width dependent manner. However, the mechanism of how visible femtosecond laser affects the viability of different microorganisms is still elusive. In this report, the cellular surface properties, membrane integrity and metabolic rate of *Escherichia coli* (*E.coli*) irradiated by a visible femtosecond laser ( $\lambda=415\text{nm}$ , pulse width=100fs) with different exposure time were investigated. Our results showed that femtosecond laser treatment for 60 minutes (min) led to cytoplasmic leakage, protein aggregation and alternation of the physical properties of *E. coli* cell membrane. In comparison, a 10 min exposure of bacteriatofemtosecond laser irradiation induced an immediate reduction of 75% of the glucose-dependent respiratory rate, while the cytoplasmic leakage was not detected. Results from enzymatic assays showed that oxidases and dehydrogenases involving in *E.coli* respiratory chain exhibited divergent susceptibility after laser irradiation. This early commencement of respiratory inhibition after a short irradiation is presumed to play a dominant effect on the early stage of bacteria inactivation.

**Key word:** *femtosecond lasers; bacteria inactivation; respiratory inhibition*

## 1. Introduction

Research efforts focusing on finding alternative antibacterial therapeutics have been raised due to the side effects and persisting antibiotic resistance of the clinically adopted antibiotics [1]. The application of photodynamic therapy technology on eliminating pathogenic microbials serves as a good example of a successful tactic in killing antibiotic-resistant bacteria by using a combination of photosensitizer and low intensity visible light [2]. However, side effects such as allergic dermatitis and porphyria have been reported and the carcinogenic potential of certain photosensitizers has been discovered [3, 4].

In recent years, an emerging pathogen elimination method using a visible femtosecond laser had been reported to be capable of selectively inactivating a wide spectrum of microorganisms, including bacteria, enveloped and nonenveloped viruses on a wavelength and pulse width dependent manner [5-13]. Maneuvering of this laser technology has several advantages over the other existing pathogen elimination treatments. First, it is environmentally friendly, because no introduction of chemical or nanoparticle based-reagents is needed. Second, it is a general disinfection strategy for a variety of viral and bacterial pathogens since the technology has been demonstrated to be effective on the enveloped and non-enveloped, single-stranded, double-stranded DNA or RNA viruses and gram-positive and gram-negative bacteria [14]. Third, its antimicrobial efficacy is likely as effective for the original strain as for the mutated ones because this laser strategy targets the global mechanical (vibrational) properties of microorganisms [14].

Previous study on M13 bacteriophage and murine norovirus, which are non-enveloped viruses, showed that the capsid proteins of the viruses were disintegrated by the laser irradiation [6, 13]. On the other hand, for the enveloped viruses, the experimental results indicated that the aggregation of capsid proteins and the subsequent inhibition of capsid function was the cause of the inactivation [12]. The fundamental effect a femtosecond laser exerted on these two kinds of viruses can both be attributed to the disruption of hydrogen bonds and/or hydrophobic interactions through the Impulsive Stimulated Raman Scattering (ISRS) [12, 13].

In nowadays, pathogenic bacteria have raised a public health challenge because of the development of antibiotic resistance. Previous research has suggested that the relaxation of supercoiled plasmid DNA caused by femtosecond laser treatment can induce genetic damage, resulting in the inactivation of *Salmonella typhimurium*[11]. Nevertheless, the time dependency and the inactivation mechanism of bacteria by the femtosecond laser irradiation remained unclear. In this study, the cellular surface properties, membrane integrity and metabolic rate of *Escherichia coli* (*E.coli*) irradiated by a visible femtosecond laser ( $\lambda=415\text{nm}$ ,

pulse width=100fs) with different exposure time were investigated. Our results demonstrated that the surface physical properties such as the stiffness (Young's modulus) and the adhesive force of the treated bacteria were altered when *E. coli* exposed to a femtosecond laser for 60 min. In addition, cytoplasmic leakage, protein aggregation, and shrinkage of cell volume as well as respiratory inhibition were observed with the femtosecond laser treated bacteria as well. These results suggest that membrane protein structure alteration due to protein aggregation may be the cause of cytoplasmic leakage and cell volume reduction of the laser-treated bacteria. In comparison, a 10 min exposure of bacteria to femtosecond laser irradiation induced an immediate reduction of 75% of the glucose-dependent respiratory rate, while the cytoplasmic leakage and protein aggregation were not detectable. Further enzymatic activity assays showed that the oxidases and dehydrogenases involving in *E. coli* respiratory chain demonstrated divergent susceptibility after a short femtosecond laser irradiation. This compromised respiratory enzymes functions may play a role in the early stage of bacteria inactivation by the visible femtosecond laser.

## **2. Material and Methods**

### **2.1. Bacteria Preparation and Membrane Preparation**

The TOP10 *E. coli* strain (Invitrogen) was utilized in this study. A single bacteria colony picked from LB agar plate were incubated in 4ml liquid LB at 37 °C for 16 hours, then subcultured by a 1:50 dilution in fresh LB liquid to mid-log phase and harvested by centrifuge at 5000 × g for 1 min. Cells were suspended in 1 ml phosphate buffered saline (PBS) and loaded into glass vials for the subsequent irradiation. The irradiated bacteria were diluted in series, spread on LB agar plates and incubated at 37 °C for 16 hours. The numbers of viable bacteria were counted as the numbers of colonies formed on LB plates. The membrane fractions were prepared by sonicating bacterial cells with cell disruptor following the protocol used by Lönnerdal B. et al [15]. The protein concentration was determined by Bradford assay (Bioshop).

### **2.2. Femtosecond laser irradiation**

Optical setup of femtosecond laser system is presented schematically in figure 1. The excitation source employed in this work was a diode pumped mode-locked Ti-sapphire laser. The laser produced a continuous train of about 70 fs pulses at a repetition rate of 80 MHz. The output of the second harmonic generation system at wavelength of 415nm was used to irradiate the sample. It has a maximum average power of about 250 mW and a pulse width of full-width at half maximum (FWHM)  $\cong$  100 fs. An achromatic lens was used to focus the beam into a glass vial containing bacteria suspension. An estimation of the focused spot size

is made by knife edge method. The peak power density is defined as that at the tightest focused region formed by the focusing lens. The power densities varies from  $\cong 20 \text{ MW/cm}^2$  to  $\cong 4.3 \text{ GW/cm}^2$  were achieved by adjusting the average power with a calibrated variable attenuator. All the experimental results reported here are obtained at  $T = 20^\circ\text{C}$  and with single beam excitation.

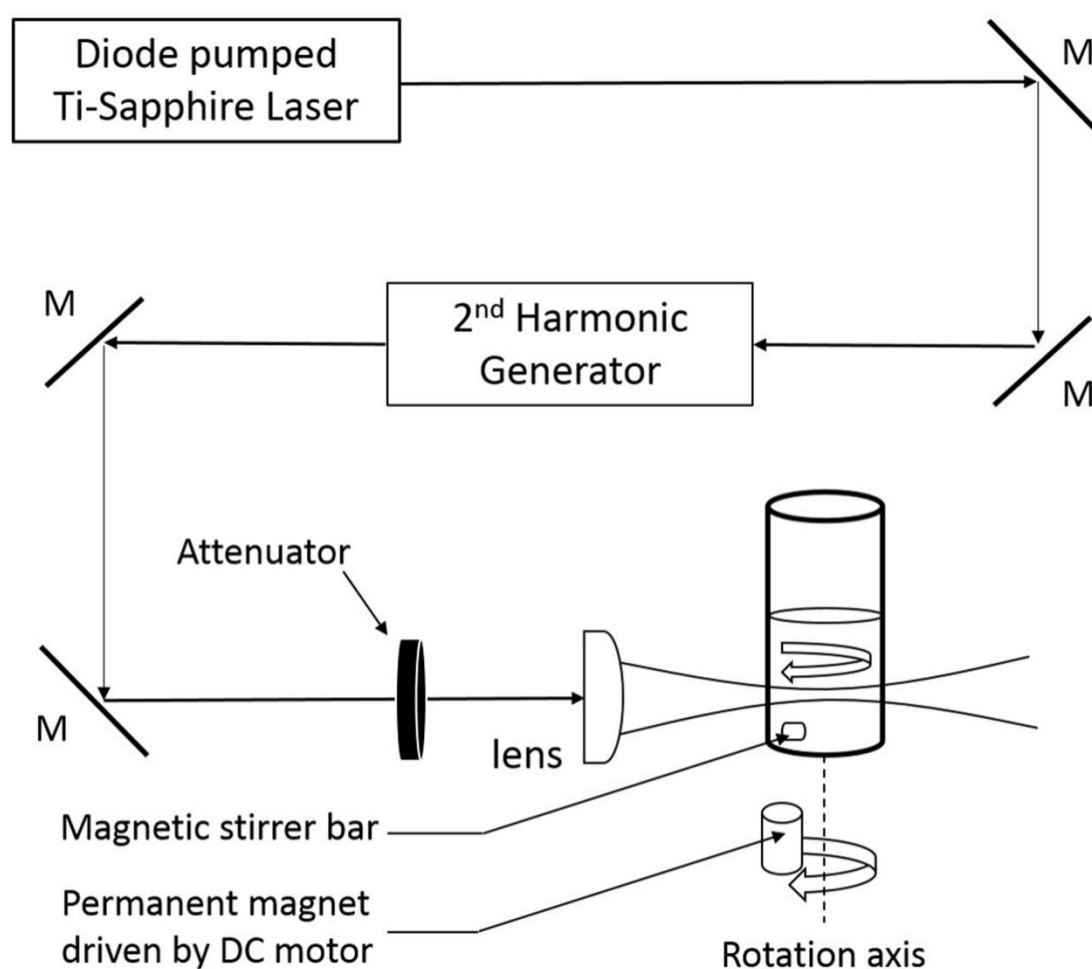


**Figure 1. Schematics of the femtosecond laser microorganism inactivation system.** The arrow denotes the propagation of the laser.

### 2.3. Spectroscopic quantification of cell leakage and florescence imaging

Irradiated or control bacteria were precipitated by centrifuge at  $5000\times g$  for 10 minutes. The supernatant was then carefully pipetted out for colorimetric measurement using NanoDrop 1000 spectrophotometer (Thermo scientific). The bacteria were stained with propidium iodide (PI, 710400 KPL) for 5 min and then observed using a florescent microscope after several washes. PI is a dye that specifically bound to DNA and excluded from viable bacteria thus the excited florescence could be used to quantify the permeability change after laser treatment. All the images were collected with Leica DM RE microscope.

#### 2.4. Protein extraction and electrophoresis

Total proteins of bacteria were extracted with B-PER protein extraction reagents (Thermo scientific). Protein concentration was determined by Bradford assay. Solutions of laser-treated or control bacteria containing equivalent quantities of protein were boiled in reducing loading buffer and separated on a 4-20% gradient express PAGE gel (Genscript). Protein bands were visualized with Coomassie blue staining (Biomann scientific).

#### 2.5. Poly-L-lysine Mica Preparation and Bacteria Immobilization

Immobilization of bacteria on poly-L-lysine treated mica is demonstrated to be a reliable method for AFM both in air and liquid [16, 17]. We followed the protocol of preparing substrate proposed by Bolshakova et al. with slight modifications [16]. To immobilize bacteria, 20  $\mu$ l of bacteria suspension were placed on mica and incubated for 20 minutes at room temperature. The mica carrying immobilized bacteria were immediately placed in a liquid cell with 0.5 ml PBS for AFM investigation.

#### 2.6. Atomic Force Microscopy (AFM)

The AFM analyses discussed in this study were all collected by using Bruker DNP-10 cantilever, with a nominal spring constant of 0.06 N/m and tip diameter of 2 nm. Young's modulus and adhesive force of the analyzed area were obtained using Bruker Multi-mode 8 atomic microscope operated in Peak Force QNM mode. The scan rate was 0.5 Hz and the maximum applied force was limited to 1 nN. Data processing and the extraction of mechanical properties are done with NanoScope Analysis from Bruker. Topographical images are presented with contrast adjustment and background removal with the open source software Gwyddion[18].

#### 2.7. Respiration assays

Respiration rates in cell suspensions were determined at 20°C by measuring oxygen consumption rate using a Clark type dissolved oxygen sensor and interface controller (CoachLab II+, CMA). Bacteria suspension were irradiated by laser for 10 minutes with a range of peak power density, or irradiated with constant power for different exposure time. Oxygen consumption rate was recorded as  $\text{mg}\cdot\text{l}^{-1}\cdot\text{min}^{-1}$  oxygen consumed after the adding of glucose in the suspensions.

#### 2.8. Oxidase & Dehydrogenase Assays

Chemicals such as Decylubiquinone (D7911), Sodium DL-lactate (71720), DL- $\alpha$ -Glycerol phosphate magnesium salt hydrate (17766),  $\beta$ -Nicotinamide adenine dinucleotide, reduced disodium salt hydrate (N8129), Sodium succinate dibasic hexahydrate (s2378),

phenazinemethosulphate (P9625), and 2,6-Dichlorophenolindophenol sodium salt hydrate (33125) used in the assays were purchased from Sigma Aldrich. The assays on oxidase and dehydrogenase activities were conducted following the procedures used by Lönnerdal B. et al [15]. The reduction of the dichlorophenol-indophenol indicator was monitored to determine the activities of dehydrogenases, and the oxidases activities were determined by measuring the oxygen consumption rate while the different substrates were added. Prepared membrane fractions irradiated for 10min were chosen to examine the enzyme activities in respiratory chain.

### 3. Experimental Results

#### 3.1. Inactivation of *Escherichia coli* by 415nm femtosecond laser

In our study, we tested the effect of femtosecond laser on the viability utilizing a 415 nm, 100 fs laser source. The load reduction depends on the power density as well as the exposure time (Data not shown). We have found that a load reduction as large as 3 in  $\log_{10}$  scale of viability was observed after 1 hour irradiation.

#### 3.2. Femtosecond laser irradiation alters the surface physical property of bacteria

To investigate the membrane integrity and cell topography after 1 hour laser irradiation, we adopted AFM to evaluate the cellular volume, height, rigidity and adhesiveness of the bacteria before and after irradiation. As can be seen in figure 2(a), untreated *E. coli* cells are appeared in rod shape. In comparison, the topology of laser irradiated bacteria looked similar to the control except that their cell volume and height were significant decreased (figure 2(b) and 2(c)). Specifically, the volume of cell shrinks from  $1.78 \pm 0.85$  to  $0.79 \pm 0.35 \mu\text{m}^3$ , and the average cell height decreases from  $516 \pm 99$  to  $394 \pm 98$  nm. The mechanical properties of bacterial surface were probed by AFM tip and the results demonstrated that there are considerable differences between the irradiated and control. As can be seen in figure 2(d) and 2(e), the Young's modulus of control ( $1.27 \pm 0.46$  Mpa) is significantly lower than the Young's modulus of irradiated bacteria ( $3.00 \pm 0.72$  Mpa), and the adhesive force of control ( $0.33 \pm 0.13$  nN) is notably higher than the adhesive force of irradiated bacteria ( $0.20 \pm 0.12$  nN).

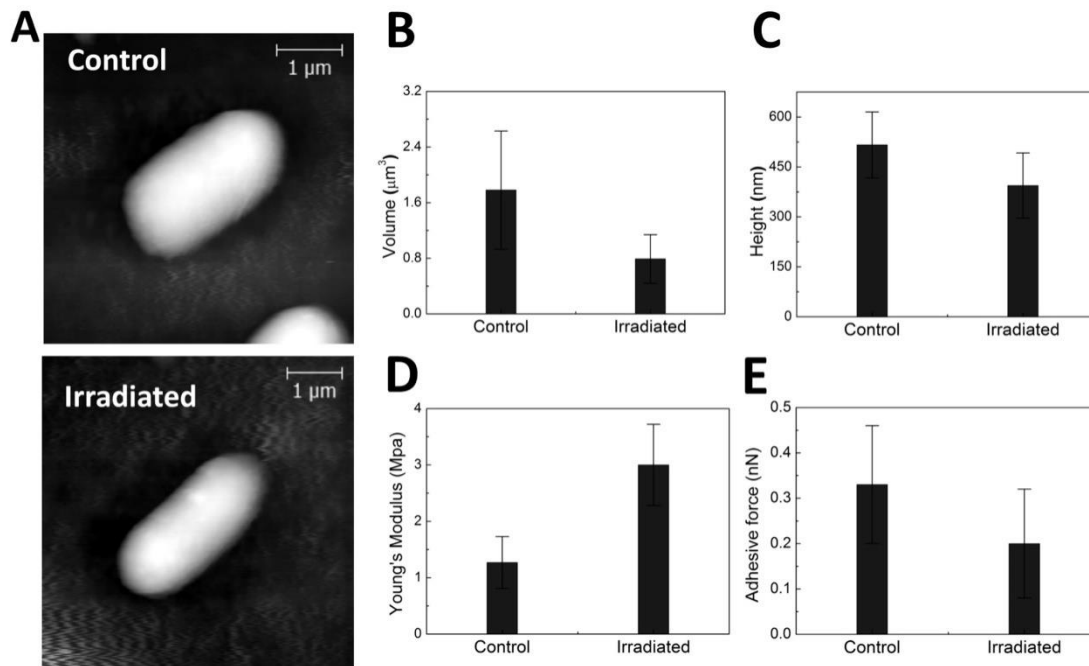


**Figure 2. Exposure to femtosecond laser caused alteration of cell surface physical properties.** (A) AFM topography images of control (top) and laser irradiated (bottom) *E. coli*. The summarized topographical properties in (B) cell volume, (C) average cell height and mechanical properties, (D) Young's modulus and (E) adhesive force are presented respectively.

### 3.3. Femtosecond laser irradiation caused leakage of bacterial cellular substances

To investigate the cause of viability reduction after 1 hour laser treatment, we adopted fluorescence imaging and absorption spectroscopy to detect the leakage of cellular substances of the laser-irradiated bacteria. The bacteria exposed to 1hr laser irradiation (figure 3(a)-(h)) shown a strong fluorescence from PI intercalating nucleic acids relative to the untreated bacteria (figure 3(i)-(p)). The counts of the bacteria with definite and distinguishable fluorescent images in a  $20 \times 20 \mu\text{m}^2$  frame was found dependent to the laser irradiation time (figure 3(q)). Number of PI stained bacteria increased from  $1.6 \pm 1.4$  (control)  $15.5 \pm 2.5$  of the bacteria exposed to laser for 60min. The optical density of the supernatant of the centrifuged bacteria suspension at the wavelength of 260 nm and 280 nm shown in figure 3(r) corresponds to the absorption of nucleic acids and proteins, respectively. The power density dependent leakage of nucleic acids and proteins is shown in the figure inset, which indicates that the laser-induced cellular substance leakage increases as the power density increases. These results strongly suggest that the integrity of the cell membranes was compromised after 1 hour laser treatment.

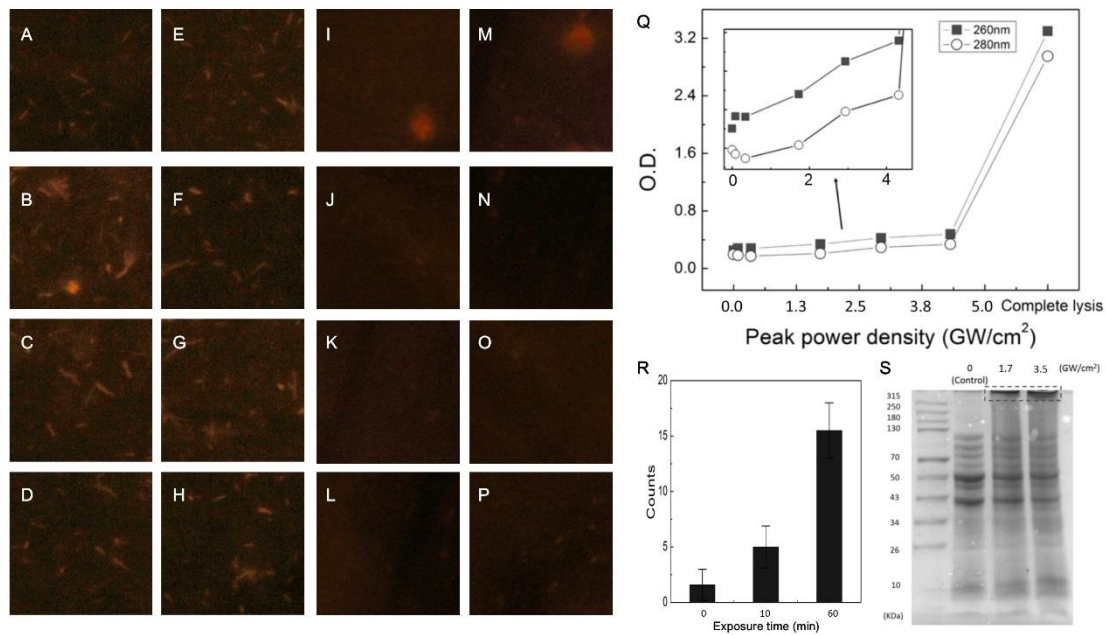


**Figure 3. Exposure to femtosecond laser caused *E. coli* cellular nucleic acid leakage and protein aggregation.** Represent florescent images of PI stained bacteria exposed to 1hr laser irradiation (A-H) and the untreated bacteria (I-P) are shown. (Q) Optical density of the media from the irradiated bacteria at 260nm (■) and 280nm (○). The inset is the enlargement of the segment of the optical density curve between 0 to 4.3 GW/cm<sup>2</sup>. The counts of the detectable bacteria florescence signals are presented in (R). Image from coomassie blue stained SDS-PAGE (S) containing total proteins extracted from control (lane 2) or irradiated (lane 3 and 4) protein sizes are indicated by the size marker (unit in KDa) in Lane 1.

### 3.4. Femtosecond laser irradiation alters bacterial protein expression profile

To investigate whether 1 hour laser treatment of *E. coli* changed the total protein expression profile, total proteins from control and treated bacteria were separated and visualized using SDS-PAGE technique [12]. As indicated in the dotted rectangular box in figure 3(s), while majority of the protein bands from the irradiated groups showed reduced intensity, the high molecules weight protein aggregations appeared on the top of the electrophoresis wells, and the intensity of the aggregated protein band increases as the power density increases. This result demonstrated that, similar to the visible femtosecond laser treated virus [12], protein aggregation occurred after bacteria were exposed to laser irradiation.

### 3.5. Short time femtosecond laser exposure affects bacterial respiratory rate

Both previous reports [12] and this study demonstrated that protein aggregation occurs after microorganisms were irradiated with femtosecond laser for 1 hr or longer. However, whether

shorter femtosecond laser irradiation time affects bacterial normal physiological activities is not known. To investigate the effect of shorter laser irradiation on bacteria, we measured the oxygen consumption rates for the control and laser-irradiated bacteria because glucose-dependent aerobic respiration rate can directly reflect the bacterial physiological state.

In figure 4(a), the respiratory rates are plotted as a function of the exposure time of laser irradiation at a constant peak power density of 2.8 GW/cm<sup>2</sup>. The respiratory activity descends rapidly despite a relatively low laser fluence applied. An over 50% decrease of the respiration rate is reached in less than 10 minutes of irradiation. The dependence of respiratory rate to peak power density is exhibited in figure 4(b). The respiration is quickly suppressed when exposing to laser with peak power larger than 0.2 GW/cm<sup>2</sup>. Therefore, the aerobic respiratory rate is immediately affected after a brief femtosecond laser irradiation. In addition, no significant change of membrane permeability between bacteria exposed to 10min laser irradiation and the control samples (cytoplasmic leakage assay in figure 4(c) and PI incorporation assay in figure 4(d)-4(i)).

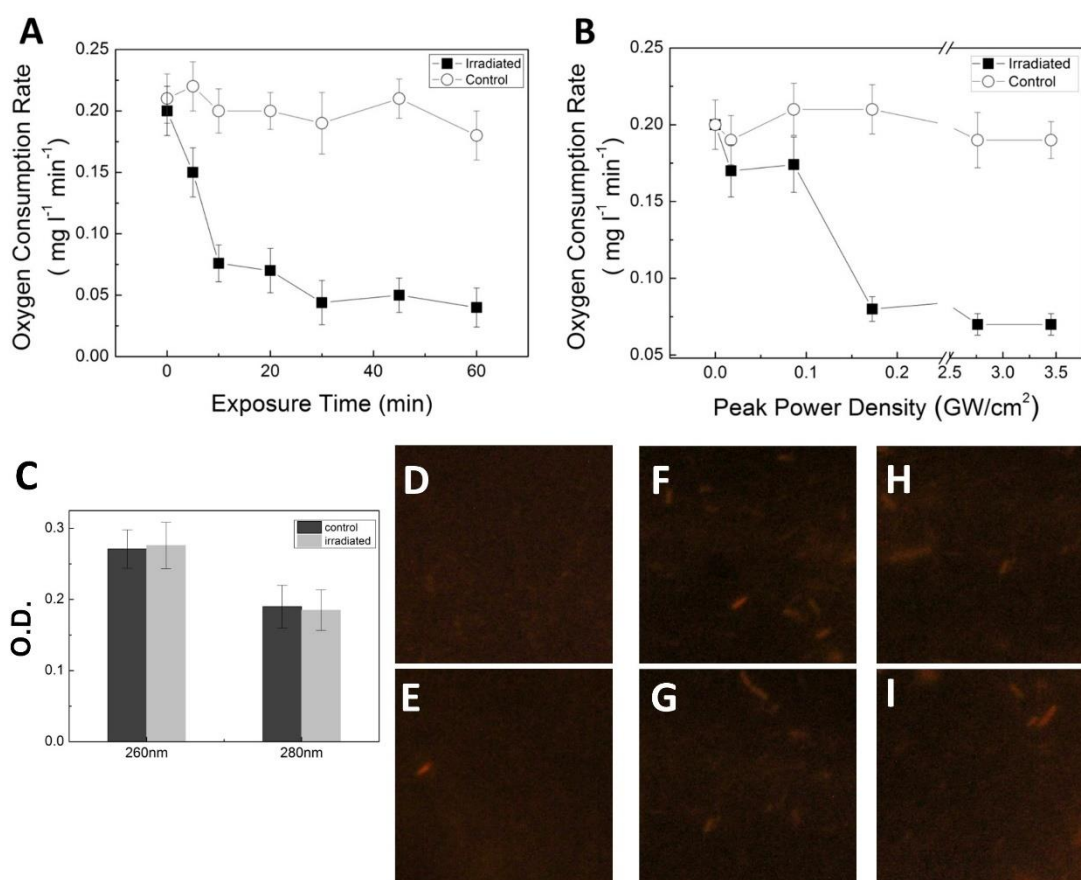


**Figure 4. Immediate reduction of cell respiratory rate followed short exposure to femtosecond laser.** (A-B) The oxygen consumption rate of the control (○) and the irradiated

sample (■) are plotted as a function of exposure time at a constant peak power density of 2.8 GW/cm<sup>2</sup> (in A), or as a function of power density (in B). (C) The absorption spectra at 260nm and 280nm (O.D.<sub>260,280</sub>) of supernatant from bacteria suspension irradiated by laser for 10 min. The absorbance in the control and irradiated samples are identical within the error. (D-I) Florescent image of PI stained bacteria of the control group (D,E) and the bacteria exposed by 10 min laser irradiation (F-I).

### 3.6. Effects of the femtosecond laser on membrane-associated respiratory enzymes

To understand whether quick inactivation of membranes-associated respiratory enzymes through laser-induced molecular vibration in *E. coli* (ISRS effect) [12] accounts for the reduction of respiratory rate, the DCPIP (dichlorophenol-indophenol) oxidoreduction reaction assays were performed with the membrane fractions extracted from irradiated and control bacteria. Utilizing different electron donors to trigger the reduction of DCPIP by each corresponding dehydrogenases, our results indicated that the dehydrogenases from the irradiated groups (denoted as open legends) could not efficiently reduce the DCPIP as their counterparts from the control groups (filled legends) did (figure 5(a)-5(b)). Interestingly, while the succinate, DL-lactate, and glycerol-3-phosphate dehydrogenases are 41.3±2.6%, 42.1±2.6% and 20.1±7.4% reduced respectively, 87.6±3.5% of the NADH dehydrogenase activities from the irradiated bacteria remained (figure 5(a)-5(b)). In comparison, the oxygen consumption rates from the irradiated groups (denoted as open legends) were greatly inactivated comparing to their counterparts from the control groups (filled legends), where 61.4±8.9% of the succinate; 63.9±5.7% of glycerol-3-phosphate, 61.2±7.1% of the DL-lactate, and 46.5±4.8% of the NADH oxidase activities were reduced respectively (figure 5(c)-5(d)). In addition, the inactivation of terminal oxidase activity measured using Decylubiquinone (reduced DB), a ubiquinone analogue, was 69.5±7.2% to the control (figure 5(c)-5(d)). The notable decrease of the terminal oxidase activity indicated a disruption of electron transport train at the level of using the reduced equivalents of the quinone.

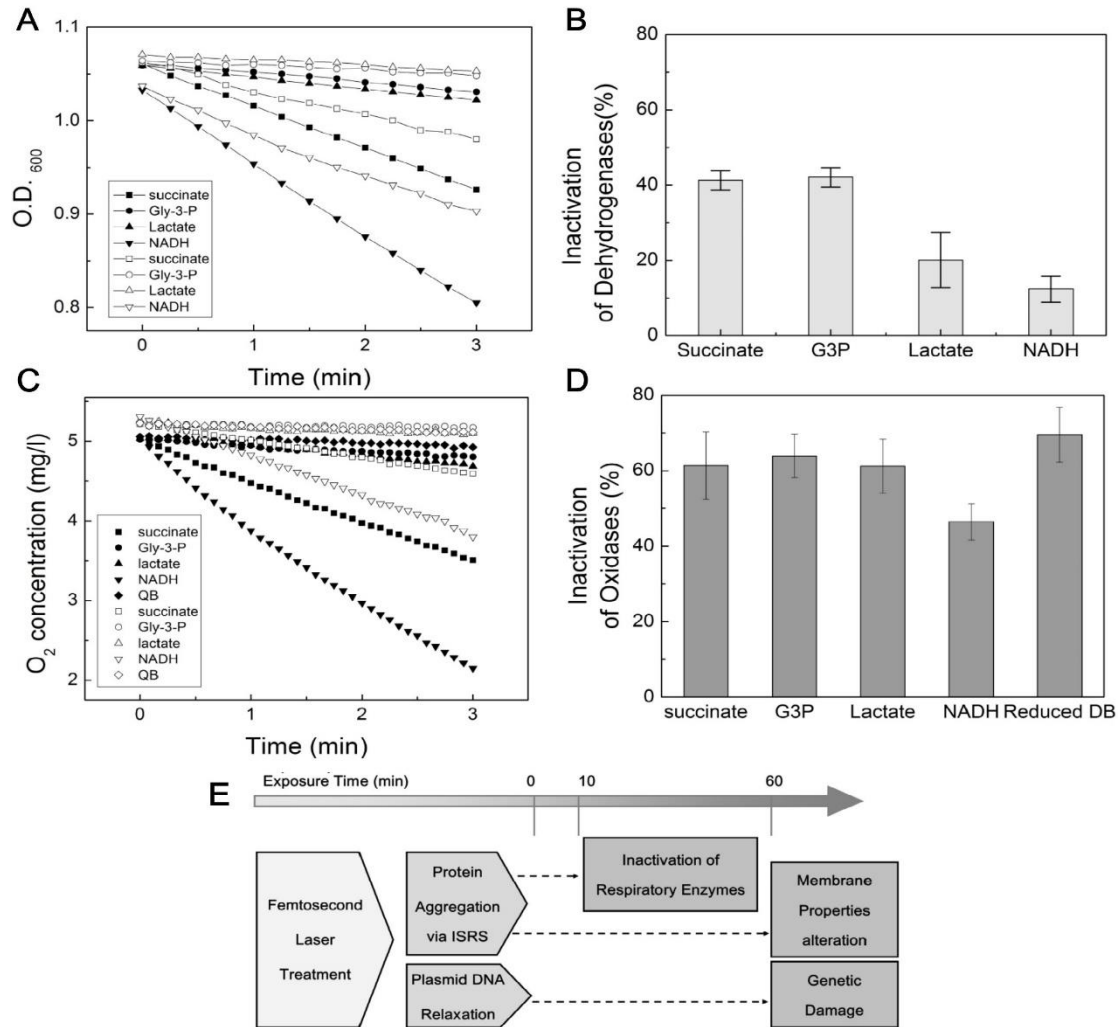


**Figure 5. Effect of the femtosecond laser on respiratory enzymes.** (A-B) DCPIP reduction assays on the membrane-associated respiratory dehydrogenase. Degree of DCPIP reduction is reflected by the absorbance at 600nm (O.D.<sub>600</sub>) and were plotted as the function of time (in A), the degree of dehydrogenase activity reduction is calculated (in B). (C-D) The dissolved oxygen concentrations were measured and presented as a function of time (in C); and the degree of oxidase activity reduction is calculated (in D). The untreated groups were denoted as filled symbols and the laser irradiated groups were denoted as open ones in (A) and (C). (E) A pictorial model of the interaction between femtosecond laser and *E. coli*. The upper arrow denotes the time scale of the interaction and lower square specifies the activated events in the bacterial inactivation.

#### 4. Discussion

In this report, we demonstrated that irradiation for 1 hour with a femtosecond laser having a wavelength centered at 415 nm, pulse width of 100 fs and the power density equal to

3.1GW/cm<sup>2</sup> can efficiently inhibit bacteria growth. Utilizing AFM to evaluate the physical property of irradiated bacteria, we found that their cellular volume, height, rigidity (stiffness) as well as the adhesiveness were altered (figure 2(b)-2(e)). Utilizing permeability assay and absorption spectroscopy to detect the nucleic acid and protein amount in the media, we found that the membrane permeability of irradiated bacteria is altered (Figure 3(a)-(r)).

In the AFM examination, the decrease of cell volume after femtosecond laser irradiation is significant. However, we did not detect the appearance of large amount of DNA and proteins in the supernatant of the irradiated bacteria, indicating that the materials leaking out could primarily be water and cellular ions. One feature worth notice is that the amount of the leaking substances is relatively low when comparing to the totally lysed bacteria. This observation indicates that the membranes can still restrain most of the large biomolecules after 1 hour laser treatment when the power density is below 4.3 GW/cm<sup>2</sup>. However, cellular ion balance is essential for maintaining proper cellular functions, such as the control of turgor pressure and solute transport. Therefore, the increased permeability could become a detrimental effect to the normal metabolism of irradiated bacteria. Another observation from AFM examination is that although there is no observable defect or indentation on the membrane surface (figure 2(a)), the increase of surface stiffness (Young's modulus) suggested that an alteration of membrane structure was induced by the laser irradiation, because change of Young's modulus reflects the conformational change of the extracellular layer and the dimensional change of periplasmic space that are sensitive to the internal structural details of cellular materials [19]. Furthermore, because prior reports indicated that the decrease of the adhesion force on both Gram-negative and positive bacteria cell surfaces after antibacterial photodynamic therapy or environmental pH alteration reflects the destruction of envelope polymers and the exposure of proteins inside the envelope [19, 20], the decrease of adhesiveness of the laser irradiated *E. coli* in our study thus further suggested that laser irradiation induced structural alteration of the bacteria membrane. Consistent with this notion, the results from the permeability assay indeed indicated that the integrity of the cell membranes was compromised after 1 hour laser irradiation.

In our case of femtosecond laser irradiated bacteria, the alteration of membrane structural integrity could be related to the aggregation of membrane proteins. Utilizing gel electrophoresis (SDS-PAGE) to separate and visualize the total protein expression of irradiated bacteria, we found that similar to the femtosecond laser treated virus [12], the high molecules weight protein aggregations appeared indeed, and the intensity of the aggregated protein band increases as the laser power density increases (figure 3(s)). Because the 415nm femtosecond laser adopted in this study lacks enough photon energy to excite the covalent bond formation in bacterial proteins [12], the disruption of weak bonds and the

partial-unfolding of proteins by the ISRS-mediated coherent molecular vibrations are the possible causes of the protein aggregation observed in this study. In addition, because the permeability and the cell surface physical properties are maintained and regulated by the structural and chemical composition of cell membranes, the alteration of membrane structure caused by protein aggregation might be the cause for the releasing of the cellular substances.

The test of glucose-dependent respiration is often adopted as an assay to examine the damage of membrane structure, which eventually leads to cytoplasmic leakage and a lethal effect to bacteria [21-23]. In this study, we tested whether a shorter irradiation could affect the glucose-dependent respiratory rate. The results showed that the inhibition of respiration, the decrease of oxygen consumption, is triggered when exposing bacteria suspension to the power density greater than  $0.2 \text{ GW/cm}^2$ . The respiratory rates remained on 25% to the control regardless the further increasing of power density or exposure time (figure 4(a), 4(b)). Because the laser-induced genetic damages would require a longer period of time to become effective [11], this early commencement of respiratory inhibition after a shorter exposure time might be caused by the inactivation of respiratory enzymes through laser-induced molecular vibration that blocked the energy uptake process and interrupt metabolism in *E. coli*. Consistently with this notion, the membrane-associated dehydrogenases and oxidases showed various degrees of inhibition (figure 5(a)-5(d)). Nevertheless, in the assay of dehydrogenases, the NADH dehydrogenase activity showed only 12.4% inactivation by the laser irradiation. On the other side, the NADH oxidase inactivation abruptly increased to 46.5%. The significant difference between the extents of inactivation might be explained by the selective inactivation of the quinone reduction subunit in the NADH dehydrogenase [15]. It suggests that the laser irradiation could cause local alteration on the enzyme complex. Also, the effect femtosecond laser deposited to the enzyme might be dependent to the species of enzymes and the subunit composition.

## 5. Conclusions

In this study, we have demonstrated that the femtosecond laser irradiation-induced *E. coli* inactivation is a combined effect of an early respiratory rate reduction and the later cell permeability, membrane structure and genetic damages resulted from the laser irradiation-induced protein inhibition via ISRS process. A schematic drawing describes the relationship between irradiation time and bacteria state is presented in figure 5(e). The proposed scenario is that a brief femtosecond laser irradiation directly inhibits the enzyme functions in the aerobic respiratory chain and causes an immediate oxygen consumption reduction within the irradiated bacteria. This compromised respiratory function may play a role in the early stage of bacteriainactivation by the femtosecond laser treatment. The effect is

not only immediate but also can be activated with a very low laser power. As the exposure time increases, the other detrimental factors such as genetic damages and the alteration of membrane surface properties will contribute to the inactivation and induce a high reduction of viability. The future research focusing on how a brief femtosecond laser irradiation immediately affects the cellular respiratory system shall reveal the structure of proteins in the enzyme complex that are highly sensitive to the ISRS-mediated coherent molecular vibrations. The identification of the specific enzyme targets in respiratory chain of the femtosecond laser irradiation may contribute to the development of a new strategy to the pathogen elimination technology.

### **Acknowledgments**

The authors are grateful for the insightful discussion with Dr. Chia-Ho Shih (IBMS, Academia Sinica, Taiwan), and the financial support from the National Science Council (NSC) of Taiwan (Republic of China), grant numbers 99-2112-M003-004-MY3 and 102-2112-M003-011.

## References

- [1] Hamblin M R and Hasan T 2004 Photodynamic therapy: a new antimicrobial approach to infectious disease? *Photochemical & photobiological sciences : Official journal of the European Photochemistry Association and the European Society for Photobiology***3** 436-50
- [2] Kashef N, Ravaei Sharif Abadi G and Djavid G E 2012 Phototoxicity of phenothiazinium dyes against methicillin-resistant *Staphylococcus aureus* and multi-drug resistant *Escherichia coli* *Photodiagnosis and Photodynamic Therapy***9** 11-5
- [3] Wulf H C and Philipsen P 2004 Allergic contact dermatitis to 5-aminolaevulinic acid methylester but not to 5-aminolaevulinic acid after photodynamic therapy *British Journal of Dermatology***150** 143-5
- [4] Darlenski R and Fluhr J W 2012 Photodynamic therapy in dermatology: past, present, and future *Journal of Biomedical Optics***18** 061208-
- [5] Tsen K T, Tsen S W D, Chang C L, Hung C F, Wu T C and Kiang J G 2007 Inactivation of viruses by coherent excitations with a low power visible femtosecond laser *Virology Journal***4**
- [6] Tsen K T, Tsen S W D, Chang C L, Hung C F, Wu T C and Kiang J G 2007 Inactivation of viruses by laser-driven coherent excitations via impulsive stimulated Raman scattering process *Journal of Biomedical Optics***12**
- [7] Tsen K T, Tsen S W D, Chang C L, Hung C F, Wu T C and Kiang J G 2007 Inactivation of viruses with a very low power visible femtosecond laser *Journal of Physics-Condensed Matter***19**
- [8] Tsen K T, Tsen S W D, Sankey O F and Kiang J G 2007 Selective inactivation of micro-organisms with near-infrared femtosecond laser pulses *Journal of Physics-Condensed Matter***19**
- [9] Tsen K T, Tsen S W D, Hung C F, Wu T C and Kiang J G 2008 Selective inactivation of human immunodeficiency virus with subpicosecond near-infrared laser pulses *Journal of Physics-Condensed Matter***20**
- [10] Tsen K T, Tsen S W D, Fu Q, Lindsay S M, Kibler K, Jacobs B, Wu T C, Karanam B, Jagu S, Roden R B S, Hung C F, Sankey O F, Ramakrishna B and Kiang J G 2009 Photonic approach to the selective inactivation of viruses with a near-infrared subpicosecond fiber laser *Journal of Biomedical Optics***14**
- [11] Tsen K T, Tsen S W D, Fu Q, Lindsay S M, Li Z, Cope S, Vaiana S and Kiang J G 2011 Studies of inactivation of encephalomyocarditis virus, M13 bacteriophage, and *Salmonella typhimurium* by using a visible femtosecond laser: insight into the possible inactivation mechanisms *Journal of Biomedical Optics***16**

- [12] Tsen S W, Chapa T, Beatty W, Tsen K T, Yu D and Achilefu S 2012 Inactivation of enveloped virus by laser-driven protein aggregation *J Biomed Opt***17** 128002
- [13] Tsen S-W, Kingsley D, Poweleit C, Achilefu S, Soroka D, Wu T and Tsen K-T 2014 Studies of inactivation mechanism of non-enveloped icosahedral virus by a visible ultrashort pulsed laser *Virology Journal***11** 20
- [14] Tsen S W, Wu T C, Kiang J G and Tsen K T 2012 Prospects for a novel ultrashort pulsed laser technology for pathogen inactivation *J Biomed Sci***19** 62
- [15] Shin K, Hayasawa H and Lönnerdal B 2001 Inhibition of Escherichia coli respiratory enzymes by the lactoperoxidase-hydrogen peroxide-thiocyanate antimicrobial system *Journal of Applied Microbiology***90** 489-93
- [16] Bolshakova A V, Kiselyova O I, Filonov A S, Frolova O Y, Lyubchenko Y L and Yaminsky I V 2001 Comparative studies of bacteria with an atomic force microscopy operating in different modes *Ultramicroscopy***86** 121-8
- [17] Doktycz M J, Sullivan C J, Hoyt P R, Pelletier D A, Wu S and Allison D P 2003 AFM imaging of bacteria in liquid media immobilized on gelatin coated mica surfaces *Ultramicroscopy***97** 209-16
- [18] Nečas D and Klapetek P 2012 Gwyddion: an open-source software for SPM data analysis *Central European Journal of Physics***10** 181-8
- [19] Gaboriaud F, Dague E, Bailet S, Jorand F, Duval J and Thomas F 2006 Multiscale dynamics of the cell envelope of Shewanella putrefaciens as a response to pH change *Colloids Surf B Biointerfaces***52** 108-16
- [20] Jin H, Huang X, Chen Y, Zhao H, Ye H, Huang F, Xing X and Cai J 2010 Photoinactivation effects of hematoporphyrin monomethyl ether on Gram-positive and -negative bacteria detected by atomic force microscopy *Appl Microbiol Biotechnol***88** 761-70
- [21] Cox S D, Gustafson J E, Mann C M, Markham J L, Liew Y C, Hartland R P, Bell H C, Warmington J R and Wyllie S G 1998 Tea tree oil causes K<sup>+</sup> leakage and inhibits respiration in Escherichia coli *Lett Appl Microbiol***26** 355-8
- [22] Cox S D, Mann C M, Markham J L, Bell H C, Gustafson J E, Warmington J R and Wyllie S G 2000 The mode of antimicrobial action of the essential oil of Melaleuca alternifolia (tea tree oil) *J Appl Microbiol***88** 170-5
- [23] Cox S, Mann C, Markham J, Gustafson J, Warmington J and Wyllie S 2001 Determining the Antimicrobial Actions of Tea Tree Oil *Molecules***6** 87-91